THE JOURNAL OF PHYSICAL CHEMISTRY B

ARTICLE

pubs.acs.org/JPCB

Effect of Ionic Size on the Structure of Cylindrical Electric Double Layers: A Systematic Study by Monte Carlo Simulations and Density Functional Theory

Teena Goel, Chandra N. Patra,* Swapan K. Ghosh, and Tulsi Mukherjee

Theoretical Chemistry Section, Chemistry Group, Bhabha Atomic Research Centre, Mumbai 400 085, India

ABSTRACT: The effect of ionic size on the diffuse layer characteristics of a cylindrical electric double layer is studied using density functional theory and Monte Carlo simulations for the restricted primitive model and solvent primitive model. The double layer is comprised of an infinitely long, rigid, impenetrable charged cylinder also referred to as the polyion, located at the center of a cylindrical cell containing the electrolyte, which is composed of charged hard spheres and the solvent molecules as neutral hard spheres (in the case of the solvent primitive model). The diameters of all the hard spheres are taken to be the same. The theory is based on a partially perturbative scheme, where perturbation is used to approximate the ionic interactions and the hard sphere contribution is treated within the weighted density approach. The Monte Carlo simulations are performed in the canonical ensemble. The zeta potential profiles as a function of the polyion surface charge density are presented for cylindrical double layers at different ionic concentrations, ionic valences, and different hard sphere (ionic and the solvent) diameters of 2, 3, and 4 Å. The theory agrees quite well with the simulation results for a wide range of system parametric conditions and is capable of showing the maximum and minimum in the zeta potential value for systems having divalent counterions. The steric effects due to the presence of solvent molecules play a major role in characterizing the zeta potential and the ionic density profiles. A noticeable change in the concavity of the zeta potential plots with increasing particle size at very low concentrations of monovalent electrolytes is suggestive of the occurrence of infinite differential capacitance for such systems.

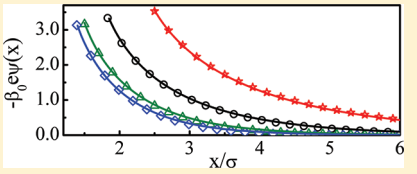

I. INTRODUCTION

The electric double layers (EDLs) at surfaces are present everywhere ranging from fundamental life processes such as the transport of ions, water, and a number of different molecules across cell membranes to the native structure of DNA and various proteins, stability of colloidal dispersions and the counterion condensation in polyelectroltes, adhesion and lubrication of surfaces, etc.[1,2] A quantitative understanding of the electric double layer is necessary to predict the influence of various control parameters on the occurrence of these phenomena. The presence of perturbation at the interface resulting in the development of net charge affects the distribution of ions in the surrounding interfacial region, which leads to the formation of electric double layers.[3,4] Over the years, a number of experimental techniques including the small-angle X-ray and neutron scattering[5,6] as well as a number of optical techniques including imaging have been used to probe the static structure of this interface.[7,8] These methods also give qualitative reflection of the interacting double layers, which can be quantitatively accessed through different force balance techniques, like the atomic force microscope, the surface force apparatus, etc. The behavior of the electrolyte near the electrode in both the Stern and the diffuse layers can also be studied from various voltage and capacitance measurement techniques. Similarly, electrodeposition and overvoltage measurements give quantitative estimation of transference numbers of ions across the electrode−electrolyte interface. The experimentally measured electrophoretic mobility of ions under an applied electric field can be used to calculate the double-layer potential near the surface. Recent advances in theoretical and simulation modeling of the electric double layers have been useful in providing the rational explanation of these experimental observations.[9]

Electric double layers have been extensively studied in various geometries, viz., planar,[10−19] spherical,[20−23] cylindrical,[24−31] and ellipsoidal, etc.,[32,33] to closely resemble the system of relevance. The cylindrical double layers represent the simplest model systems for DNA and hence are of direct relevance to electrostatic and salt effects in DNA and protein−DNA complexes. There exist several levels of theoretical descriptions of polyelectrolyte systems. The simplest approach, i.e., the restricted primitive model (RPM), of the electrolyte considers the ions as charged hard spheres of equal diameter and subsumes all solvent effects into a bulk or effective permittivity in the Coulombic interactions. Various experimental properties such as osmotic pressure, activity coefficients, or Donnan equilibria[34] have been explained in terms of very crude DNA models such as the primitive model. However, it is well-known that the ion solvation and dipole orientation of the solvent at the surface, correlated with the molecular structure of the solvent, are crucial in determining the potential and ion distributions at the surface. Inadequate treatment of the solvent is considered as severe limitation of the theoretical developments of the electric double layers.[35,36] To improve the model for EDL, the solvent

Received: April 23, 2011
Revised: August 1, 2011
Published: August 09, 2011

can be assumed as a specific molecular species. The civilized model electrolyte includes a dipolar or a multipolar solvent, but it may increase the complexity of theoretical calculation to a large extent. However, the solvent primitive model (SPM),[23,37−39] where solvent is considered as the neutral hard sphere, considers the molecular nature of the solvent while overcoming the problems associated with the solvent polarization effects. Addition of the neutral solute in polyelectrolyte solutions has been used to mimic the crowding interactions, thereby providing[40] interesting insights into the polyion−polyion and polyion−small ion correlations. The molecular nature of the solvent is crucial for explaining many experimental observations such as oscillations of the forces between two surfaces immersed in an electrolyte solution with a change in the distance between them. The detailed structure of DNA and its properties can be studied with an all-atom model through molecular dynamics simulations,[41] using more sophisticated models of the solvent, specifically that of water, which however involves huge computational requirements.

The theoretical approach provides the framework for quantitative interpretation of the structural and thermodynamic behavior of the double layers. The techniques that are employed for such studies are mostly based on classical statistical mechanics, which are classified into different categories, namely, Poisson−Boltzmann (PB) theory,[42,43] integral equation methods,[44−46] modified PB approach,[47−49] density functional theory (DFT),[17,18,20,27−29,50] and computer simulation methods.[10] The PB theory is the simplest one which takes the distribution of point ions as a Boltzmann type under the influence of the charged field. A number of modifications of PB theory have been introduced[47−49] over the decades to take into account the finite size of the ions. The Ornstein−Zernike (OZ) integral equation has been solved in various forms by taking into account a number of closure relations and different bulk correlation functions. Density functional techniques[51] are based on the minimization of grand potential with suitable approximation for the free energy functional involving perturbation or weighted density approximations. The methods based on these sophisticated approaches have revealed a number of new behaviors of the electric double layers at high concentrations and/or higher surface charges, viz., the layering and the charge inversion phenomena. Alongside the development of analytical methods, a number of Monte Carlo and molecular dynamics simulations[52] have also been recently carried out which clearly reveal these new phenomena and provide direct evidence of negative interfacial capacitance in several instances. Extensive Monte Carlo simulation studies are performed for electric double layers under the framework of simple models such as the restricted primitive model.[10,24,30,53,54] However, simulations with more complicated models such as SPM[23,38,55,56] or dipolar[57] solvent are very few due to their computer-intensive requirements.

It is now well understood that the structure of the electric double layer depends upon the competition between the electrostatic correlations and the excluded volume effects. The potential that exists at the boundary of electric double layers is known as the zeta potential. The zeta potential is important as it provides an indirect measurement of electrokinetic mobility of ions in a given solution. The magnitude of the zeta potential gives an indication of the potential stability of the colloidal system. Apart from zeta potential, the thermodynamic property "inverse differential capacity", C_d^{-1}, is of interest related to the electric double-layer phenomena. The inverse differential capacity is defined as

$$C_d^{-1} = \frac{d\psi_0}{dQ} \tag{1}$$

where ψ_0 is the total potential drop from the polyion surface (i.e., charged surface) to infinity and Q is the polyion charge density. The value of the inverse differential capacity was earlier considered to be essentially positive in the case of electric double layers.[58,59] Recently, many theoretical and simulation methods have shown that there is a definite possibility of negative value of C_d^{-1} for highly coupled systems with large polyion charges and/or multivalent electrolytes.[3,13,25,37] The occurrence of negative inverse differential capacity also depends upon the strong ion-size correlations. In the present work, we report another instance of existence of negative curvature of the zeta potential versus surface charge density plots for the cylindrical double layers for mono- and multivalent counterions with large ionic sizes at high surface charge densities.

In recent reports, the structure of cylindrical double layers (CDLs) has been studied, systematically in the framework of RPM and SPM through density functional theory and Monte Carlo simulations.[30,38,60] In this work, we present the effect of hard sphere (ionic and solvent) size variation on the zeta potential characteristics of the cylindrical double layers for both RPM and SPM using density functional theory and Monte Carlo simulations. The density functional formalism and MC simulation method are similar to the already reported studies.[30,38,60] The theory is partially perturbative, where the hard sphere interactions are calculated through weighted density approximation, using the Denton and Ashcroft recipe.[61] The Coulombic interactions are treated perturbatively around a uniform fluid and are calculated through second-order direct correlation function obtained from mean spherical approximation (MSA).[62] The interplay between the ionic correlations and excluded volume effects has been shown previously[60] to influence the characteristics of the double layer such as layering, charge inversion, etc. phenomenally. In this work, the dependence of zeta potential against the variation in the polyion surface charge density is studied at different conditions such as ionic and neutral hard sphere sizes, concentrations, and valence of the ions, etc. The theoretical predictions for the zeta potential values are shown to match the simulation results for a wide range of system parametric conditions.

Although this work is an extension of our earlier studies on CDLs, it clearly emphasizes upon the variation in zeta potential with respect to the system parameters such as ionic concentrations, valences, as well as the ionic and solvent sizes. It is quite well-known that the interaction of counterions with the polyion has a dominant effect on the double-layer characteristics, and our recent articles[30,38,60] have also shown that the interplay between the ionic and excluded volume correlations is most important in manipulating the structure of CDL. This work involving SPM further elucidates that the incorporation of neutral hard spheres as the solvent molecules (SPM) in the system affects the double-layer properties, e.g., zeta potential, in such a way that the possibility of the existence of negative differential capacitance can be introduced merely by increasing the excluded volume effects through an increase in ionic and solvent sizes, even at low ionic concentrations. The possibility of negative differential

capacitance has been shown earlier in other polyelectrolyte geometries, viz., for planar[10,13,63,64] and spherical[20,22,65] ones, but such a phenomenon has been rarely addressed in the cylindrical polyelectrolyte systems having electrolytes with the solvent as the third component.

II. THEORETICAL FORMULATION

A. Molecular Model. In this study, we consider the restricted primitive model as well as the solvent primitive model for cylindrical double layers, where a centrally located isolated, infinite, rigid, and impenetrable charged cylinder with uniform surface charge density, Q, is surrounded by the small charged (ions) and neutral (solvent in the case of SPM) hard spheres of diameter, $\sigma_\alpha = \sigma$. For simplicity, the size of the ions and the solvent is taken as the same in this study so that the neutral spheres of the solvent contribute to the excluded volume effects similar to that of the ionic species. This would avoid further complications in the model due to differences in the sizes of the counterions, co-ions, and the solvent molecules. The added advantage of having the same-sized neutral hard spheres is that we can consider them as the cosolutes and see their effect as the additional crowding effects in understanding the double-layer characteristics. The surface charge density, Q, of the polyion cylinder is given by

$$Q = \frac{e}{2\pi Rb} \tag{2}$$

where e is the electronic charge; b is the length per unit charge (inverse of linear charge density); and the radius of the polyion, R, is taken as 8 Å, to mimic the characteristics of B-DNA crudely. The dielectric constant of the medium, ε, is taken as 78.358. The height of the polyion cylinder is kept fixed, and the surface charge density is varied by suitably changing the number of charges on a fixed length of the polyion. The study is carried out for a range of hard sphere diameters, viz., $\sigma = 2$, 3, and 4 Å, and at different ionic concentrations spanning from 0.1 to 2 M for a 1:1 electrolyte and from 0.05 to 1 M for 2:1/1:2 and 2:2 electrolytes. In all cases of SPM, the concentration of the solvent is kept fixed at 10.3 M unless otherwise mentioned, which is equivalent to reduced bulk density of the solvent as $\rho_3^{0*}[=\rho_3^0\sigma^3] = 0.4$ for a hard sphere size of 4 Å. The surface charge density of the polyion, Q, is varied between 0 and 0.4 Cm^{-2}.

The total potential energy of the system is the sum of polyion−ion and ion−ion Coulombic interactions. The potential between the polyion and the small ion can thus be written as

$$U_{p\alpha}(r_\alpha) = \begin{cases} -2\dfrac{eq_\alpha}{\varepsilon b}\ln(r_\alpha), & r_\alpha \geq R + \dfrac{\sigma}{2} \\ \infty, & \text{otherwise} \end{cases} \tag{3}$$

where q_α is the charge on the ion α and r_α is its radial distance from the polyion surface. Similarly, the ion−ion potential is given as

$$U_{\alpha\beta} = \begin{cases} \dfrac{q_\alpha q_\beta}{\varepsilon r}, & r \geq \sigma \\ \infty, & \text{otherwise} \end{cases} \tag{4}$$

where r denotes the distance between two small ions, i.e., $|\mathbf{r}_\alpha - \mathbf{r}_\beta|$. The infinite potential signifies the hard-core interaction potential between the polyion and the small ions and also among all (charged and neutral) hard spheres.

B. Density Functional Theory. In classical density functional theory (DFT), the grand potential functional, Ω, is minimized with respect to the singlet density profiles, $\rho_\alpha(\mathbf{r})$, of each species, at equilibrium, to get the density distribution of individual components as well as the thermodynamic properties of the system. The density functional formalism used in the present study has been described in detail by Patra and co-workers,[27] and thus we would rather present the final expression for the density distribution of the components as a function of the radial distance from the polyion (x), which is

$$\rho_\alpha(x) = \rho_\alpha^0 \exp\{-\beta_0 q_\alpha \psi(x) + c_\alpha^{(1)\mathrm{hs}}(x;\ [\{\rho_\alpha\}]) - c_\alpha^{(1)\mathrm{hs}}([\{\rho_\alpha^0\}]) + c_\alpha^{(1)\mathrm{el}}(x;\ [\{\rho_\alpha\}]) - c_\alpha^{(1)\mathrm{el}}([\{\rho_\alpha^0\}])\} \tag{5}$$

where $\beta_0 = (k_B T)^{-1}$; k_B is Boltzmann's constant; T is the temperature, taken to be 298.15 K; $c_\alpha^{(1)\mathrm{hs}}(x; [\{\rho_\alpha\}])$ and $c_\alpha^{(1)\mathrm{el}}(x; [\{\rho_\alpha\}])$ are the hard-sphere and the electrical part of the first-order correlation function, respectively; and $\psi(x)$ represents the mean electrostatic potential of the diffused double layer due to the polyion surface charge density and the ionic distributions, given by

$$\psi(x) = \frac{4\pi}{\varepsilon}\int_x^\infty \mathrm{d}t\ t \ln\left(\frac{x}{t}\right)\sum_\alpha q_\alpha \rho_\alpha(t) \tag{6}$$

The weighted density approximation (WDA) used here is based on Denton and Ashcroft (DA)[61] to calculate $c_\alpha^{(1)\mathrm{hs}}(x; [\{\rho_\alpha\}])$, as an approximation to that of the corresponding uniform system, $\tilde{c}$, at a weighted density, $\overline{\rho}_\alpha(\mathbf{r})$, i.e.

$$c_\alpha^{(1)\mathrm{hs}}(x;\ [\{\rho_\alpha\}]) = \tilde{c}^{(1)\mathrm{hs}}(\overline{\rho}(x)) \tag{7}$$

where

$$\overline{\rho}(x) = \int \mathrm{d}t\ t w^{\mathrm{hs}}(x,t;\ \overline{\rho}(x))[\sum_\alpha \rho_\alpha(t)] \tag{8}$$

and $w^{\mathrm{hs}}(x,t)$ is the weight function obtained through DA prescription. The electrical contribution, however, is evaluated here with a perturbation around the bulk fluid given as

$$c_\alpha^{(1)\mathrm{el}}(\mathbf{r};\ [\{\rho_\alpha\}]) - c_\alpha^{(1)\mathrm{el}}([\{\rho_\alpha^0\}]) = \int \mathrm{d}\mathbf{r}' \sum_{\beta=1}^{2} \tilde{c}_{\alpha\beta}^{(2)\mathrm{el}}(|\mathbf{r}-\mathbf{r}'|; \{\rho_\alpha^0\})(\rho_\beta(\mathbf{r}') - \rho_\beta^0) \tag{9}$$

C. Monte Carlo Simulations. The standard Metropolis sampling procedure[66] for the canonical Monte Carlo (CMC) simulations (N, V, T) was adopted to obtain the structural characteristics of the cylindrical double layers (CDLs). The basic simulation cell consists of a long, rigid, hard, and uniformly charged rod passing through the center of the cylindrical sampling box.[24] The periodic boundary conditions are applied along the axial direction of the cylinder. The volume of the simulation cell is kept fixed with the height of the polyion as $2h$ and width of the simulation cell taken as R_{cell}. The cylindrical cell considered here is of central cell length ($2h$) as 68 Å, whereas the external cell length ($2l$) is taken as $14h$ to avoid end effects. The radius of the cell (R_c) is taken as 114.25 Å. Initially, the hard spheres are inserted randomly in the simulation cell and then randomly translated such that the acceptance ratio lies between 0.2 and 0.4. The total potential energy of the system is comprised of polyion−ion $U_{p\alpha}$ and ion−ion $U_{\alpha\beta}$ Coulombic interactions

along with some long-range correlations of ions outside the simulation cell. This long-range correlation effect is incorporated as a mean field term, which includes interaction of each ion with an external potential Φ_{ext} produced by the inhomogeneous charge distribution outside the cylindrical cell beyond the axial length of 2*l*. The external potential is computed self-consistently from the average charge distribution within the cell and is calculated iteratively along with the ionic distribution, $\rho(r)$, as explained in a number of earlier works.[10,24,67]

The method calculates excess energy of interaction of any ion with the external potential, Φ_{ext}, as

$$U_{ext}(r_\alpha) = q_\alpha \Phi_{ext}(r_\alpha) = (2q_\alpha/\varepsilon)\int_R^{R_{cell}} \rho_{ext}(r')B(r', r_\alpha)r'\,dr' \quad (10)$$

with $\rho_{ext}(r')$ indicating the net external charge distribution and

$$B(r', r_\alpha) = -\int_0^{2\pi} d\phi' \ln[h + \{h^2 + r_\alpha^2 + r'^2 - 2r_\alpha r' \cos\phi'\}^{1/2}] \quad (11)$$

Initially, Φ_{ext} is taken as zero, and the selection criteria for the transition probability of each move in the simulation incorporates only ion−ion and polyion−ion Coulombic interaction energies. After $\sim 10^3-10^4$ moves, the ionic density distribution thus obtained is equated to $\rho_{ext}(r')$ to evaluate the external potential at each point in the central cell. The Φ_{ext} then calculated through eq 10 is used to calculate the total configuration energy and subsequently contributes to the selection criteria of the simulation moves. The external potential is periodically recomputed from the current form of density distribution until no further changes are observed in the density distribution. The final equilibrated density distributions of all the components are obtained using block averaging over 5 blocks each having 8×10^8 moves.

III. RESULTS AND DISCUSSION

The density functional calculations and Monte Carlo simulations are performed to evaluate the structural and thermodynamical properties of cylindrical EDL. In this work, we are mainly analyzing the value of zeta potential, ζ, for CDL as a function of its surface charge density, *Q*, with variations in the ionic concentrations, valences, and the sizes of the ionic and neutral spheres. The zeta potential ζ is defined as the mean electrostatic potential (MEP) $\psi(r)$ at the distance of closest approach between a small ion and the polyion, i.e., $\zeta = \psi(R + \sigma/2)$. This gives a measure of the thickness of the EDL region in which the total charge is locally nonzero. It can be calculated using the ionic density distribution $\rho_\alpha(r)$ such as

$$\zeta = \frac{4\pi e}{\varepsilon}\int_{R+\sigma/2}^{\infty} dr \sum_\alpha z_\alpha \rho_\alpha(r)\left(r - \frac{r^2}{R + \sigma/2}\right) \quad (12)$$

Figure 1(a)−(e) presents the plot of ζ of CDL against the surface charge density Q of the polyion having 1:1 electrolyte solution for both RPM and SPM as predicted by DFT and simulations. In this case, the diameter of the small ion (and that of solvent, in the case of SPM) is varied, ranging from 2, 4, 6, 8, and 9 Å. The ζ values are shown in millivolts units. The ionic concentration is taken to be 0.1 M. In this work, we are interested

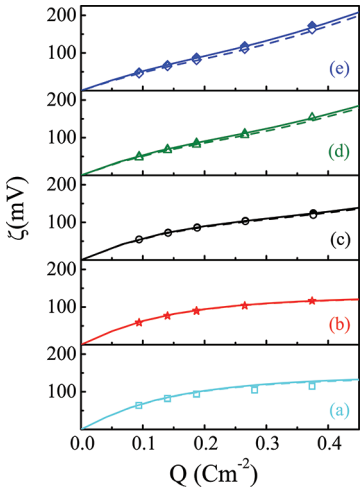

Figure 1. Zeta potential values ζ (mV) as a function of surface charge density Q (Cm^{-2}) of CDL having 1:1 electrolyte at c = 0.1 M for σ = (a) 2.0 Å (cyan, □), (b) 4.0 Å (red, ★), (c) 6 Å (black, ○), (d) 8 Å (green, Δ), and (e) 9 Å (blue, ◇). Solid and empty symbols show simulation results for RPM and SPM, respectively, while solid and dashed lines represent DFT results for RPM and SPM, respectively.

to keep the number of ions in a given cell volume fixed, so that the differences in the density profiles, the mean electrostatic potential profiles, as well as in zeta potential values can be understood as the direct outcome of only the size variations and thus the excluded volume effects of the constituent components. To emphasize the constant number of ions and solvent molecules taken in a simulation box (instead of taking constant packing fraction), we would mention all the concentrations of the components in units of molarity rather than using the reduced density. The reduced density of the components ρ_α^* (defined as $\rho_\alpha\sigma^3$) depends upon the diameter of the components σ; thus, for 0.1 M electrolyte, ρ_α^*(ions) = 0.0014 for 2 Å size, and it would be 0.13 for the 9 Å electrolyte. The reduced density values signify the packing fractions of components. Increasing the size of the fixed number of components in a fixed volume increases the packing fraction of the components (by the factor of σ^3) and reflects the increased steric interactions between the ionic and neutral components. The concentration of solvent is kept very low which is 0.3 M because of the difficulty associated with accommodating a large number of 8 or 9 Å components in a simulation box of finite dimensions and its efficient sampling. Thus, it was a compromise to take the solvent in the moderate concentrations to do the simulations efficiently and also to incorporate sufficient steric interactions.

The value of zeta potential starts increasing with an increase in the surface charge density for all the hard sphere sizes. In the case of 2 and 4 Å sizes, the curve reaches a plateau at a higher value of Q, which however starts increasing drastically at large Q values for the system with 8 and 9 Å spheres. The plot shows an interesting phenomenon where the curvature of the zeta potential versus surface charge density plot changes its sign with an increase in the hard sphere size from 4 to 6 Å. The ζ versus Q plot shows monotonically increasing trend for 2 and 4 Å sizes, while the curve assumes upward concavity in the case of hard sphere sizes of 6, 8, and 9 Å.

The ζ versus Q plot indicates the possibility of negative differential capacitance even for low concentrations of 1:1

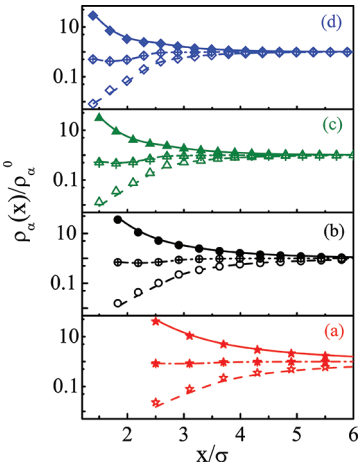

Figure 2. Comparison of density profiles of 1:1 electrolyte having 0.1 M bulk concentration for SPM around (negatively charged) DNA with different values of σ = 4.0 Å (red, ★), 6 Å (black, ○), 8 Å (green, Δ), and 9 Å (blue, ◇). Symbols are simulation results, and lines represent theoretical predictions. (Solid symbols, solid lines) represent counterions, (symbols with cross in between, dash-dotted lines) represent solvent, and (empty symbols, dashed lines) correspond to co-ions.

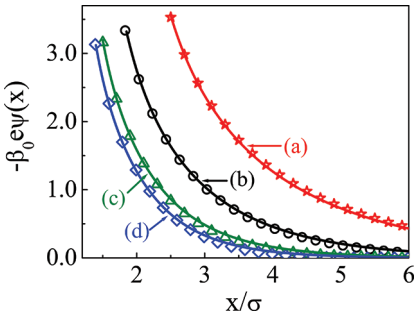

Figure 3. Mean electrostatic potential (in reduced units) profiles for 0.1 M 1:1 electrolyte in SPM with different values of σ = 4.0 Å (red, ★), 6 Å (black, ○), 8 Å (green, Δ), and 9 Å (blue, ◇). Symbols are simulation results, and lines represent theoretical predictions.

electrolytes having large size components and at high surface charge densities. The reason for change in the sign of the derivative of the slope can be attributed to the strong excluded volume effects due to larger ionic and solvent sizes that dominate over the electrostatic correlations. The similar change in concavity of ζ versus Q plots has previously been reported for spherical double layers at very large macroparticle sizes[68] and also for planar double layers for larger small ions.[10] The monotonic behavior of 2 and 4 Å electrolytes in RPM has been previously reported by Patra and Bhuiyan[29] for CDL; this result is equally interesting as it shows that even in the presence of strong excluded volume effects of solvent molecules the ionic interactions predominate in both RPM and SPM for smaller sized components (ions and solvent). The values of zeta potential are slightly less for SPM than the corresponding values in RPM for 8 and 9 Å sizes. With the introduction of solvent molecules, the ions and the solvent molecules are pushed toward the polyion surface to efficiently utilize the bulk space, which causes strong layering of the ions and the solvent at the surface, resulting in efficient surface charge screening and thus reduction of the diffused layer width. The increased layering effects neutralize the polyion charge more efficiently at smaller distances thus leading to the lower zeta potential values. The simulation results significantly match the theoretically calculated values even for larger hard sphere sizes.

Figures 2(a)−(d) and 3(a)−(d) show the representative plots of singlet density distribution function of each component and the mean electrostatic potential profiles of CDL, respectively, for 0.1 M 1:1 electrolyte in SPM at varying hard sphere (ionic and neutral) diameters, viz., 4, 6, 8, and 9 Å. The density distribution of ions are obtained by solving eq 5 iteratively, and the mean electrostatic potential is calculated using eq 6. The bulk density of the solvent is taken as 0.3 M in the case of SPM. We see the monotonic variation of density profiles, viz., accumulation of counterions as well as depletion of co-ions near the polyion. There is an appearance of a hump in the co-ion profile at a distance of ∼1σ away from the first ionic layer for systems having hard spheres of diameter 8 and 9 Å. This is due to stronger volume exclusion effects in the case of larger spheres. To maintain clarity in the figures, we have not shown the RPM results here, as the density and the MEP profiles do not show any striking differences between RPM and SPM. The similarity in the RPM and SPM results is due to the very low concentration of the ions and the solvent in the system. The MEP profiles decay monotonically as a function of distance from the surface. The decay is much faster for systems with larger components (i.e., larger ions and solvent molecules) showing the stronger screening effects of the larger ions at the surface. The predictions for density profiles of all components and that of MEP profiles from the theory and simulations compare quite well with each other.

Figures 4(a)−(c) to 6(a)−(c) show the ζ versus Q plots for CDL systems having 1:1 electrolyte in the concentration range of 0.1−2 M, while 2:1/1:2 and 2:2 electrolytes are taken in the concentration range of 0.05−1 M. The surface charge density Q is varied from 0 to 0.4 Cm^{-2}. The hard sphere diameters are taken as 2, 3, and 4 Å. In the case of SPM, the bulk concentration of the solvent is taken to be constant, i.e., 10.3 M, for all the cases mentioned here, which is equivalent to reduced bulk density of the solvent as $\rho_3^{0^*}$ = 0.4 for the hard sphere size of 4 Å, $\rho_3^{0^*}$ = 0.17 for 3 Å, and $\rho_3^{0^*}$ = 0.05 for 2 Å. By keeping the reduced density of the solvent fixed, the numbers of solvent molecules would increase enormously high for 2 and 3 Å cases; however, our intention was to study the effect of variations in ionic concentrations, keeping the solvent concentration same. The zeta potentials for the CDL system immersed in 1:1 electrolyte solution are plotted as a function of surface charge density Q in Figures 4-(a)−(c) for three sets of concentrations (c, viz., 0.1, 1, and 2 M) and for three ionic diameters (σ = 2, 3, and 4 Å). At low concentration of c = 0.1 M, the dependence of ζ on ionic diameter is quite weak; i.e., the system does not show large variations in the values of the zeta potential with change in the size, whereas at higher concentrations (c = 1 and 2 M), the magnitude of the zeta potential decreases for a given surface charge density as the size of the ions and the solvent increases. The strength of ζ decreases with salt concentration at all ionic diameters. The value of ζ is always lower for SPM than RPM due to stronger size correlations. The differences in the ζ values for RPM and SPM increase for CDL with larger hard spheres as compared to the system with smaller hard spheres. The DFT predictions agree quite well with the simulation results with slight discrepancies at very low ionic concentrations especially for smaller hard sphere (viz., 2 Å) sizes.

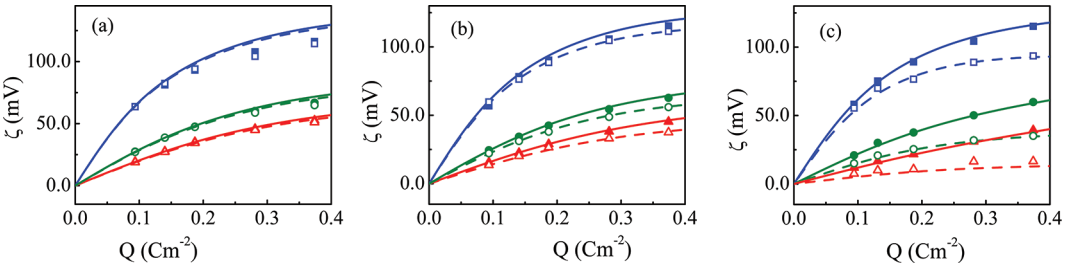

Figure 4. Zeta potential values ζ (mV) as a function of surface charge density Q (Cm^{-2}) of CDL at different 1:1 electrolyte concentrations of 0.1 M (blue, □), 1 M (green, ○), and 2 M (red, Δ) for hard sphere diameters of (a) 2 Å, (b) 3 Å, and (c) 4 Å. Solid and empty symbols show simulation results for RPM and SPM, respectively, while solid and dashed lines represent DFT results for RPM and SPM, respectively.

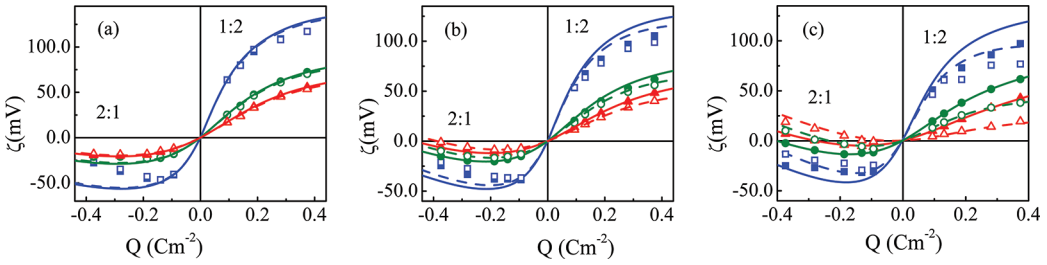

Figure 5. Zeta potential values ζ (mV) as a function of surface charge density Q (Cm^{-2}) of CDL for 2:1/1:2 electrolyte concentrations of 0.05 M (blue, □), 0.5 M (green, ○), and 1 M (red, Δ) at different values of σ (a) 2 Å, (b) 3 Å, and (c) 4 Å. The key is the same as in Figure 4.

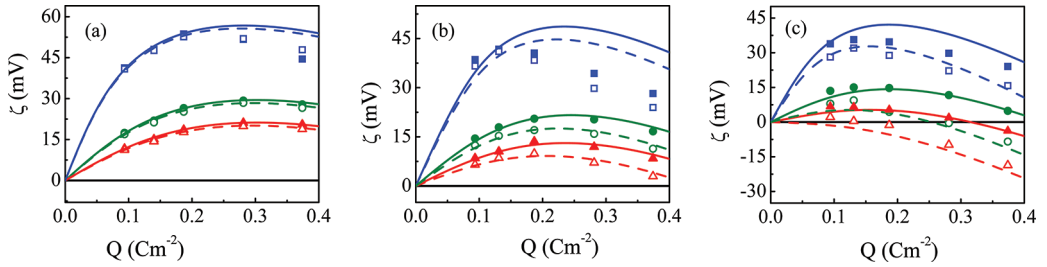

Figure 6. Zeta potential values ζ (mV) as a function of surface charge density Q (Cm^{-2}) of CDL having 2:2 electrolyte at 0.05 M (blue, □), 0.5 M (green, ○), and 1 M (red, Δ) concentrations and for σ = (a) 2 Å, (b) 3 Å, and (c) 4 Å. The key is the same as in Figure 4.

In Figures 5(a)−(c) the zeta potential ζ as a function of surface charge density Q is shown for 2:1/1:2 electrolytes of concentrations 0.05, 0.5, and 1 M for varying hard sphere sizes of 2, 3, and 4 Å. The behavior of the plot for the 1:2 electrolyte (monovalent counterions) is similar to that of the 1:1 electrolyte where the value of ζ increases monotonically with an increase in value of Q and the dependence of zeta potential upon ionic and solvent diameters is very weak. The similarity in 1:1 and 1:2 plots is due to the significance of monovalent counterions at the surface in calculation of the zeta potential values. In the case of multivalent counterions, the behavior of the zeta potential changes drastically. It is to be noted that the plot for 2:1 electrolytes is on the negative side of the quadrant. The figure shows that the ζ value depends strongly upon the ionic diameter for the 2:1 electrolyte containing divalent counterions, and the magnitude of zeta potential decreases sharply with an increase in hard sphere size. The ζ versus Q plot shows a maximum for all ionic concentrations for a larger hard sphere size of 3 Å. This maximum is not very strong in the case of CDL with smaller spheres of diameter 2 Å. The occurrence of a maximum in the ζ versus Q plot leads to the possibility of a negative differential capacitance and also implies the existence of infinite capacitance before becoming negative. In the case of CDL having a high ionic concentration of the 2:1 electrolyte with large hard sphere size (viz., 4 Å), the zeta potential changes its sign from negative to positive at high values of Q. The change in sign at larger value of surface charge density is a consequence of excess accumulation of counterions at the surface leading to a phenomenon called charge reversal. The ζ versus Q plot for SPM lies below the RPM plot, and the difference between SPM and RPM widens for systems with larger (ionic and solvent) hard spheres. Larger size implies greater adsorption of components to the surface because the system needs to push more large ions to the interface to gain accessible volume. The theoretical predictions of zeta potential values agree satisfactorily with the simulation results for the 2:1/1:2 system for all hard sphere sizes except in the case of a low electrolyte concentration of 0.05 M. It is worthwhile to mention here that DFT does not show a finite, nonzero potential of zero

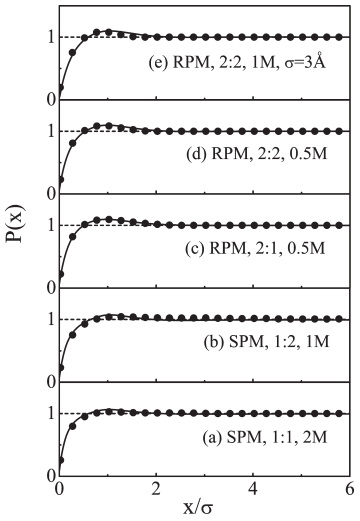

Figure 7. Charge compensation function profiles for electrolyte solutions around the (negatively charged) polyion, for (a) SPM, 1:1, 2 M, (b) SPM, 1:2, 1 M, (c) RPM, 2:1, 0.5 M, (d) RPM, 2:2, 0.5 M, and (e) RPM, 2:2, 1 M with $\sigma = 3$ Å. Symbols are simulation results, and lines represent theoretical predictions.

charge, although MC simulations do indicate a charge separation at the highest concentration of 1 M.

Figures 6(a)−(c) depict the zeta potential profiles for 2:2 electrolyte systems of CDL having the electrolyte of different concentrations, i.e., 0.05, 0.5, and 1 M, for three different ionic and solvent sizes of 2, 3, and 4 Å. The behavior of the plot is similar to that of the 2:1 electrolyte system where the zeta potential increases with increasing surface charge density Q, goes through a maximum, and then again goes down. This trend is attributed to the dominance of divalent counterions at the surface. In this case, also the effect of size variation on the zeta potential plots with respect to the surface charge density is significant. For the ionic and neutral hard sphere size of 4 Å, the zeta potential for the concentrated system (1 M) at higher Q is even negative. The possibility of a negative ζ value increases in the case of SPM due to stronger excluded volume effects of solvent molecules leading to increased layering of ions at the surface. The DFT results closely match with the simulation data at larger ionic diameters (σ) as well as at higher surface charge density (Q).

The density oscillations and charge layering in a double-layer system can be better understood in terms of the charge compensation function $P(x)$ given as[69]

$$P(x) = 2\pi b \int_0^x \sum_\alpha q_\alpha \rho_\alpha(x') x' \mathrm{d}x' \qquad (13)$$

$P(x)$ basically represents the integrated charge of the small ions within the annular volume of radial extent r and axial extent b of the polyion. To satisfy the electroneutrality condition, $P(x)$ should finally gives rise to unit charge within the length b of the polyion at the bulk limit of ionic densities. This is depicted in Figures 7(a)−(e) under various parametric conditions. In RPM as well as SPM, the presence of multivalent counterions introduces charge inversion because charge correlations gets stronger [Figures 7(a)−(d), σ = 4 Å]. Here again, the behavior of the system is in accordance with the counterions; i.e., the 1:1 system behaves like 1:2 and 2:1 like 2:2. Even at small ionic sizes, the charge correlations get preference over the size correlations as can be seen for the 1 M solution of 2:2 electrolyte with $\sigma = 3$ Å. In all the cases, however, the diffuse double-layer width remains almost the same, indicating that the charge inversion is visible only in the first layer. The theory and the simulation results match satisfactorily in all these profiles.

IV. CONCLUDING REMARKS

The structure of the cylindrical double layer is studied here using density functional theory and Monte Carlo simulations using both RPM and SPM to gain insight into the zeta potential profile as a function of polyion surface charge density for different hard sphere sizes of ions and solvent molecules. Although a number of such studies have been attempted in different times, systematics of the effect of ionic size in CDL are quite relevant in present times. We noticed a distinct change in the sign of the curvature of the zeta (ζ) versus surface charge density (Q) plot with an increase in the hard sphere (ionic and neutral) sizes for a 1:1 electrolyte at a low electrolyte concentration of 0.1 M in both RPM and SPM. At small hard sphere sizes of 2 and 4 Å, the plot reaches a plateau at high values of charge density, while for 8 and 9 Å sizes, the value of zeta starts increasing drastically at higher polyion charge density. This behavior may be attributed to the dominance of excluded volume interactions over the electrostatic interactions at larger sizes of ions and solvent molecules. The upward concavity of the $\zeta-Q$ plot indicates the possibility of negative differential capacitance.

The zeta potential profile as a function of surface charge density is also studied for the 1:1 electrolyte at three concentrations, viz., 0.1, 1, and 2 M, and for 2:1/1:2 and 2:2 electrolyte systems having concentrations of 0.05, 0.5, and 1 M, all at three different hard sphere diameters of 2, 3, and 4 Å. The behavior of 1:1 and 1:2 electrolytes is the same due to prevalence of monovalent counterions. The value of ζ depends weakly on ionic diameter at low electrolyte concentrations. However, in the case of 2:1 and 2:2 electrolytes, the magnitude of the zeta potential decreases drastically with an increase in the hard sphere size. For systems with divalent counterions, the zeta potential profile shows a maximum indicating the possibility of negative diffuse layer capacitance. This maximum is stronger in the case of large hard sphere sizes, i.e., 4 Å as compared to 2 and 3 Å sizes. The value of zeta potential becomes negative at high surface charge density for higher concentrations of larger ionic and hard sphere components. In all cases, the theoretical predictions match closely with the simulation values. A good solvent model, which can account for the appropriate relative permittivity, will be an important input in the present work. An interesting future study will be the application of the present method to the ionic density distributions at an interface carrying different surface charge distributions in layers.[70]

AUTHOR INFORMATION

Corresponding Author

*Also at Homi Bhabha National Institute (HBNI), Mumbai. E-mail: chandra@barc.gov.in.

ACKNOWLEDGMENT

The authors thank S. K. Sarkar for his interest and encouragement. The authors gratefully acknowledge support from the INDO-EU project MONAMI on Computational Materials Science.

REFERENCES

(1) Bockris, J.O'M.; Reddy, A. K. N. *Modern Electrochemistry 1: Ionics*; Plenum Press: New York, 1998.
(2) Vold, R. D.; Vold, M. J. *Colloid and Interface Chemistry*; Addison Wesley: Reading MA, 1983.
(3) Carnie, S. L.; Torrie, G. M. *Adv. Chem. Phys.* **1984**, *56*, 141.
(4) Hansen, J. P.; Löwen, H. *Annu. Rev. Phys. Chem.* **2000**, *51*, 209.
(5) Bhuiyan, L. B.; Outhwaite, C. W.; van der Maarel, J. R. C. *Phys. A* **1996**, *231*, 295.
(6) Zakharova, S. S.; Egelhaaf, S. U.; Bhuiyan, L. B.; Outhwaite, C. W.; Bratko, D.; van der Maarel, J. R. C. *J. Chem. Phys.* **1999**, *111*, 10706.
(7) Israelachvili, J. *Intermolecular and Surface Forces*; Academic Press: New York, 1992.
(8) *Imaging of Surfaces and Interfaces*; Lipkowski, J., Ross, P., Eds.; Wiley-VCH: New York, 1999.
(9) Levin, Y. *Rep. Prog. Phys.* **2002**, *65*, 1577.
(10) Torrie, G. M.; Valleau, J. P. *J. Chem. Phys.* **1980**, *73*, 5807. *J. Phys. Chem.* **1982**, *86*, 3251.
(11) Groot, R. D. *Phys. Rev. A* **1988**, *37*, 3456.
(12) Groot, R. D.; Van Der Eerden, J. P. *J. Electroanal. Chem.* **1988**, *247*, 73.
(13) Mier-y-Teran, L.; Suh, S. H.; White, H. S.; Davis, H. T. *J. Chem. Phys.* **1990**, *92*, 5087.
(14) Patra, C. N.; Ghosh, S. K. *J. Chem. Phys.* **1994**, *100*, 5219. *J. Chem. Phys.* **1994**, *101*, 4143.
(15) Boda, D.; Henderson, D.; Plaschko, P.; Fawcett, W. R. *Mol. Simul.* **2004**, *116*, 7170.
(16) Bhuiyan, L. B.; Outhwaite, C. W. *Phys. Chem. Chem. Phys.* **2004**, *6*, 3467.
(17) Pizio, O.; Patrykiejew, A.; Sokolowski, S. *J. Chem. Phys.* **2004**, *121*, 11957.
(18) Boda, D.; Fawcett, W. R.; Henderson, D.; Sokolowski, S. *J. Chem. Phys.* **2002**, *116*, 7170.
(19) Patra, C. N.; Ghosh, S. K. *Phys. Rev. E* **1993**, *47*, 4088.
(20) Yu, Y.-X.; Wu, J.; Gao, G.-H. *J. Chem. Phys.* **2004**, *120*, 7223.
(21) Guerrero-García, G. I.; González-Tovar, E.; Lozada-Cassou, M.; Guevara-Rodríguez, F. de J. *J. Chem. Phys.* **2005**, *123*, 034703.
(22) Goel, T.; Patra, C. N. *J. Chem. Phys.* **2007**, *127*, 034502.
(23) Patra, C. N. *J. Phys. Chem. B* **2009**, *113*, 13980.
(24) Mills, P.; Anderson, C. F.; Record, M. T., Jr. *J. Phys. Chem.* **1985**, *89*, 3984.
(25) González-Tovar, E.; Lozada-Cassou, M.; Henderson, D. *J. Chem. Phys.* **1985**, *83*, 361.
(26) Outhwaite, C. *J. Chem. Soc., Faraday Trans. 2* **1986**, *82*, 789.
(27) Patra, C. N.; Yethiraj, A. *J. Phys. Chem. B* **1999**, *103*, 6080.
(28) Wang, K.; Yu, Y.-X.; Gao, G.-H. *Phys. Rev. E* **2004**, *70*, 011912.
(29) Patra, C. N.; Bhuiyan, L. B. *Condens. Matter Phys.* **2005**, *8*, 425.
(30) Goel, T.; Patra, C. N.; Ghosh, S. K.; Mukherjee, T. *J. Chem. Phys.* **2008** *129*, 154906.
(31) Patra, C. N.; Yethiraj, A. *Biophys. J.* **2000**, *78*, 699.
(32) Rickayzen, G. *J. Chem. Phys.* **1999**, *111*, 1109.
(33) Bulavchenko, A. I.; Batishchev, A. F.; Batishcheva, E. K.; Torgov, V. G. *J. Phys. Chem. B* **2002**, *106*, 6381.
(34) Katchalsky, A. *Pure Appl. Chem.* **1971**, *26*, 327.
(35) Mott, N. F.; Watts-Tobin, R. J. *Electrochim. Acta* **1961**, *4*, 79.
(36) Verwey, E. J. W. ; Overbeek, J.Th., G. *Theory of the stability of lyophobic colloids*; Elsevier: Amsterdam, 1948.
(37) Tang, Z.; Scriven, L. E.; Davis, H. T. *J. Chem. Phys.* **1992**, *97*, 494.
(38) Goel, T.; Patra, C. N.; Ghosh, S. K.; Mukherjee, T. *J. Chem. Phys.* **2008**, *129*, 154707.
(39) Lamperski, S.; Pluciennik, M. *Mol. Simul.* **2010**, *36*, 111.
(40) Bhuiyan, L. B.; Vlachy, V.; Outhwaite, C. W. *Int. Rev. Phys. Chem.* **2002**, *21*, 1.
(41) Beveridge, D. L.; Ravishanker, G. *Curr. Opin. Struct. Biol.* **1994**, *4*, 246.
(42) Bloomfield, V. *Biopolymers* **1991**, *31*, 1471.
(43) Petris, S. N.; Chan, D. Y. C.; Linse, P. *J. Chem. Phys.* **2003**, *118*, 5248.
(44) *Fundamentals of Inhomogeneous Fluids*; Henderson, D., Ed.; Dekker: New York, 1992.
(45) Lozada-Cassou, M.; Saavedra-Barrera, R.; Henderson, D. *J. Chem. Phys.* **1982**, *77*, 5150.
(46) Lozada-Cassou, M. *J. Phys. Chem.* **1983**, *87*, 3729.
(47) Das, T.; Bratko, D.; Bhuiyan, L. B.; Outhwaite, C. W. *J. Phys. Chem.* **1995**, *99*, 410.
(48) Das, T.; Bratko, D.; Bhuiyan, L. B.; Outhwaite, C. W. *J. Chem. Phys.* **1997**, *107*, 9197.
(49) Bhuiyan, L. B.; Outhwaite, C. W. *J. Chem. Phys.* **2002**, *116*, 2650.
(50) Ni, H.; Anderson, C. F.; Record, M. T., Jr. *J. Phys. Chem. B* **1999**, *103*, 3489.
(51) Evans, R. In *Fundamentals of Inhomogeneous Fluids*; Henderson, D., Ed.; Dekker: New York, 1992.
(52) Allen, M. P.; Tildesley, D. J. *Computer Simulation of Liquids*; Oxford University Press: New York, 1987.
(53) Degrève, L.; Lozada-Cassou, M. *Mol. Phys.* **1995**, *86*, 759.
(54) Terao, T.; Nakayama, T. *Phys. Rev. E* **2001**, *63*, 041401.
(55) Zhang, L.; Davis, H. T.; White, H. S. *J. Chem. Phys.* **1993**, *98*, 5793.
(56) Boda, D.; Henderson, D.; Patrykiejew, A.; Sokolowski, S. *J. Chem. Phys.* **2000**, *113*, 802.
(57) Boda, D.; Chan, K.-Y.; Henderson, D. *J. Chem. Phys.* **1998**, *109*, 7362.
(58) Blum, L.; Lebowitz, J. L.; Henderson, D. *J. Chem. Phys.* **1980**, *72*, 4249.
(59) Landau, L. D. ; Lifshitz, E. M. *Electrodynamics of Continuous Media*; Pergamon: Oxford, 1960; Chap. 3.
(60) Goel, T.; Patra, C. N.; Ghosh, S. K.; Mukherjee, T. *J. Chem. Phys.* **2010**, *132*, 194706.
(61) Denton, A. R.; Ashcroft, N. W. *Phys. Rev. A* **1991**, *44*, 8242.
(62) Waisman, E.; Lebowitz, J. L. *J. Chem. Phys.* **1972**, *56*, 3086. **1972**, *56*, 3093.
(63) Lozada-Cassou, M.; Henderson, D. *J. Phys. Chem.* **1983**, *87*, 2821.
(64) Goel, T.; Patra, C. N.; Ghosh, S. K.; Mukherjee, T. *Mol. Phys.* **2009**, *107*, 1.
(65) Modak, B.; Patra, C. N.; Ghosh, S. K.; Vijayasundar, J. *Mol. Phys.* **2011**, *109*, 639.
(66) Metropolis, N.; Rosenbluth, A. W.; Rosenbluth, M. N.; Teller, A. H.; Teller, E. *J. Chem. Phys.* **1953**, *21*, 1087.
(67) Murthy, C.; Bacquet, R. J.; Rossky, P. J. *J. Phys. Chem.* **1985**, *89*, 701.
(68) González-Tovar, E.; Jimènez-Àngeles, F.; Messina, R.; Lozada-Cassou, M. *J. Chem. Phys.* **2004**, *120*, 9782.
(69) Montoro, J. C. G.; Abascal, J. L. F. *J. Chem. Phys.* **1995**, *103*, 8273.
(70) Wang, Z.; Ma, Y. *J. Chem. Phys.* **2009**, *131*, 244715.